The X-shooter pipeline

Andrea Modigliani[a], Paolo Goldoni[b],[c] Frederic Royer[d], Regis Haigron[d], Laurent Guglielmi[b], Patrick François[d], Matthew Horrobin[e], Paul Bristow[a], Joel Vernet[a], Sabine Moehler[a], Florian Kerber[a], Pascal Ballester[a], Elena Mason[f], Lise Christensen[g].

[a]European Southern Observatory, ESO, Karl Schwarzschild-Str. 2a, D-85748, Garching, Germany;
[b]Laboratoire AstroParticule et Cosmologie, 10 rue A. Domon et L. Duquet,75205 Paris Cedex 13, France;
[c]DSM/IRFU/Service D'Astrophysique, CEA-Saclay, 91191 Gif-sur-Yvette, France;
[d]GEPI/UMR 8111, Observatoire de Paris, 11 avenue M. Berthelot, 92195 Meudon Cedex, France;
[e]Univ. zu Köln, Address, Köln, Germany;
[f]European Southern Observatory, Alonso de Cordova 3107 Vitacura, Santiago, Chile;
[g]Excellence Cluster Universe, Universität München, Boltzmann-str.2, 85748 Garching, Germany.

ABSTRACT

The X-shooter data reduction pipeline, as part of the ESO-VLT Data Flow System, provides recipes for Paranal Science Operations, and for Data Product and Quality Control Operations at Garching headquarters. At Paranal, it is used for the quick-look data evaluation. The pipeline recipes can be executed either with EsoRex at the command line level or through the Gasgano graphical user interface. The recipes are implemented with the ESO Common Pipeline Library (CPL).

X-shooter is the first of the second generation of VLT instruments. It makes possible to collect in one shot the full spectrum of the target from 300 to 2500 nm, subdivided in three arms optimised for UVB, VIS and NIR ranges, with an efficiency between 15% and 35% including the telescope and the atmosphere, and a spectral resolution varying between 3000 and 17,000. It allows observations in stare, offset modes, using the slit or an IFU, and observing sequences nodding the target along the slit.

Data reduction can be performed either with a classical approach, by determining the spectral format via 2D-polynomial transformations, or with the help of a dedicated instrument physical model to gain insight on the instrument and allowing a constrained solution that depends on a few parameters with a physical meaning.

In the present paper we describe the steps of data reduction necessary to fully reduce science observations in the different modes with examples on typical data calibrations and observations sequences.

Keywords: Astronomical Data Reduction, Echelle and IFU data reduction, Instrument Physical Modelling.

1. INTRODUCTION

The Pipeline Systems Department of the Software Development Division at ESO is responsible for the development of instrument data reduction pipelines[1].[2] Pipelines are used by Paranal and La Silla operations as quick-look tools to do a real-time coarse assessment of the quality of calibrations and science observations. When the data arrive at ESO Garching (generally within one hour), a more thorough data processing and evaluation is performed by the Quality Control (QC) group. Here, the pipeline is used to automatically process raw calibration frames into master calibrations, generate quality control parameters in order to monitor the telescope, instrument, and detector performance, and to assess the quality of the calibrations and science observations.[3]

Further author information: (Send correspondence to A.M.)
A.M.: E-mail: amodigli@eso.org, Telephone: +49 (0)89 320 06 789

The X-shooter pipeline is based on the data reduction library developed by the X-shooter consortium with contributions from France, The Netherlands and ESO.[4] Finally, the pipelines are also released to the public to allow any instrument or archive user to do a data reduction optimised to their science case. The X-shooter pipeline as well as other VLT instrument pipeline releases are publicly available at www.eso.org/pipelines.

X-shooter is a single target spectrograph for the Cassegrain focus of Kueyen. It is the first of the second generation instruments at the ESO Very Large Telescope. The instrument covers in a single exposure the spectral range from the UV to the K band (300-2500 nm). It is designed to maximize the sensitivity in this spectral range through the splitting in three arms (UVB, VIS, NIR) with optimised optics, coatings, dispersive elements and detectors. It operates at intermediate resolutions (R=3000-17,000, depending on wavelength and slit width) with fixed echelle spectral format (with prism cross-dispersers) in the three arms. The possibility to observe in a single shot at the sky limit faint sources with an unknown flux distribution has inspired the name of the instrument.

At the entrance of each spectrograph there is a slit unit equipped with 11" long slits of different widths. The light coming from the telescope after the focus is directed to the UVB and VIS arms and transmitted to the NIR spectrograph cryostat by two dichroic in series. It is also possible to use an image slicer in the focal plane that reformats a 1.8"×4" field of view on the sky into a 0.6"×12" long slit. In slit mode it is possible to correct atmospheric dispersion effects by inserting an ADC unit in the UVB and VIS arm optical paths. Flexures are actively compensated by piezo-controlled mirrors. X-shooter started commissioning in November 2008, had Science Verifications in the summer 2009 and is operational since 1st October 2009.[5]

2. DATA REDUCTION MODES

The X-shooter data reduction can be performed in two modes: polynomial, where order centre and slit or ifu edges trace and the 2D transformation that allows removal of the order curvature and the spectral line tilt are expressed as small degree polynomials; physical model, where the position on the detector of any wavelength/slit position can be obtained using a physical model of the instrument characterized by several parameters that describe the orientations, locations and other physical properties of the optical components of the spectrograph.[6]

Both approaches are calibrated via the matching of lines observed in an arc lamp multi-pinhole exposure to catalogue wavelengths. In the case of the polynomial method, a low order polynomial is fit to obtain an empirical dispersion solution. A sufficient density of calibration lines is required in each order, the polynomial coefficients have no physical meaning and the fit cannot be reliably extrapolated far outside of the region where the lines were identified. Nevertheless, this is the classical, tried and tested approach, the formulation adopted describes well X-shooter's complex spectral format and the pipeline executes somewhat quicker in this mode.

The physical model method, on the other hand, utilizes an optimisation algorithm to adjust parameters until the physical model, reproduces all the observed positions of the arc lamp lines simultaneously. This approach is less constrained by the local density of calibration lines and has some predictive power. Moreover, the parameters have physical meaning which make them useful for instrument monitoring and for understanding phenomena such as flexure[7] and changing environmental conditions.[3] Consequently this approach is used by QC.

3. X-SHOOTER DATA REDUCTION CHALLENGES

X-shooter can observe simultaneously with three channels and generate three sets of frames for its UVB, VIS and NIR arms (see Fig. 1). In order to fully reduce a set of X-shooter data, including calibration and science frames, the following data reduction problems need to be solved: If needed (after macro-Earthquake events) determine a proper instrument model configuration that describes the current X-shooter spectral format.[8] Determine the following detector quantities: bias, dark current, linearity and gain both globally and locally. Compute a global wavelength and slit calibration. Correct for instrument flexures. Perform the sky subtraction in all observation modes. 2D rectification. Optimal extraction. Efficiency and response determination. 3D cube reconstruction for observations in IFU mode. Error propagation and bad pixel flagging through all the relevant steps.

The pipeline has to address all those challenges in a robust, automatic and accurate manner and provide not only products required to perform the full data reduction chain and analyse science data but also additional
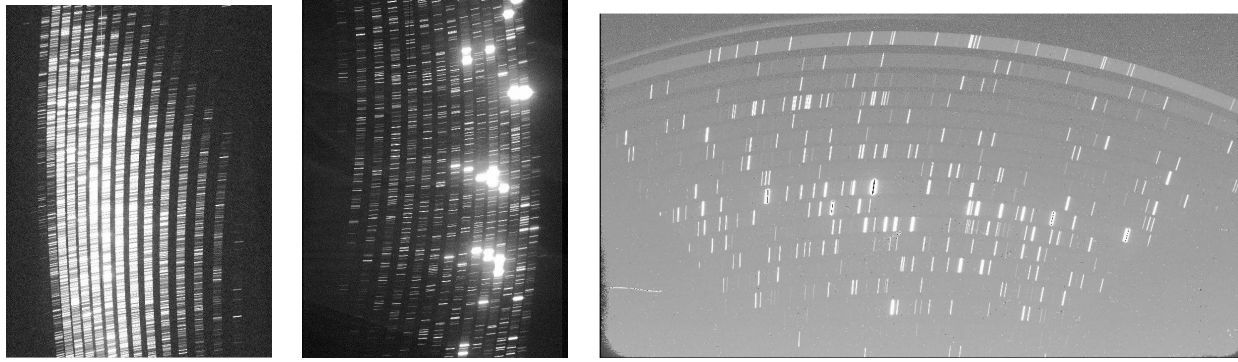
Figure 1. This image displays left to right the XSH UVB, VIS and NIR spectral formats with different image scales.

products for quality control. This pipeline provides also a set of useful scripts to effectively check the accuracy of the main data reduction steps.

4. DATA REDUCTION CASCADE

Initially the raw frames are prepared by trimming pre-scan and over-scan regions. In order to have a common spectral format layout and facilitate the following data reduction the data are re-oriented to the VIS raw data orientation. Two extensions are associated with each frame, one containing the corresponding error image and the other a qualifier image flagging bad pixels of different nature. For each input raw frame, the error frame is calculated from the raw counts (transformed in electrons using read noise and gain) contained in each pixel. The error and bad pixel frames are propagated throughout the data reduction cascade.

4.1 Detector linearity characterization

For UVB and VIS arm, this recipe processes a set of flat frames acquired with increasing exposure time and a set of bias frames and, for NIR arm, a set of lamp-on and lamp-off frames acquired with increasing detector integration time. In UVB and VIS arms, the intrinsic detector contribution can be removed by subtracting from each flat frame the master bias obtained by median stack-combine the bias frames while, in NIR arm, by subtracting from each flat lamp-on exposure the corresponding lamp-off one. Then, using the so-called Photon Transfer Curve (PTC) method, this data reduction step determines the range of exposure times and detector count levels within which the detector response can be considered linear. The locations of detector pixels that have a non-linear responsivity are stored in a image, the non-linear bad pixel map. This recipe allows also to measure the detector gain that is proportional to the slope of the PTC. The non-linear pixels map is one of the most important maps to be included in the master bad pixel map used to reduce science NIR data.

4.2 Bias frames processing

UVB and VIS bias frames are median stack-combined and a master frame is determined with removal of contributions from outlier counts via a standard kappa sigma clipping technique. Low counts and high counts pixels locations are indicated in the corresponding bad pixel maps. For quality control the detector read out noise, the master bias fixed pattern noise and its X and Y structures (see Fig. 2, left), that are the collapsed frame spectrum standard deviations after collapsation of the frame along Y and X direction, are determined.

4.3 Dark frames processing

UVB and VIS dark frames are not used in the data reduction, as the correction is very small, unless the user has very long exposure science observations. Dark frames are median stack-combined and a master frame is generated and normalized to one second exposure, with cosmic ray hits (CRHs) and noisy pixels flagging and removal via standard kappa sigma clipping technique. The noisy pixels and CRHs locations are stored in corresponding maps. Processing the NIR master dark frame it is possible to determine the corresponding detector read out noise, the fixed pattern noise and the detector contamination. The noisy pixel map, in NIR arm, provides an important contribution to the master bad pixel map to be used for science data reduction.
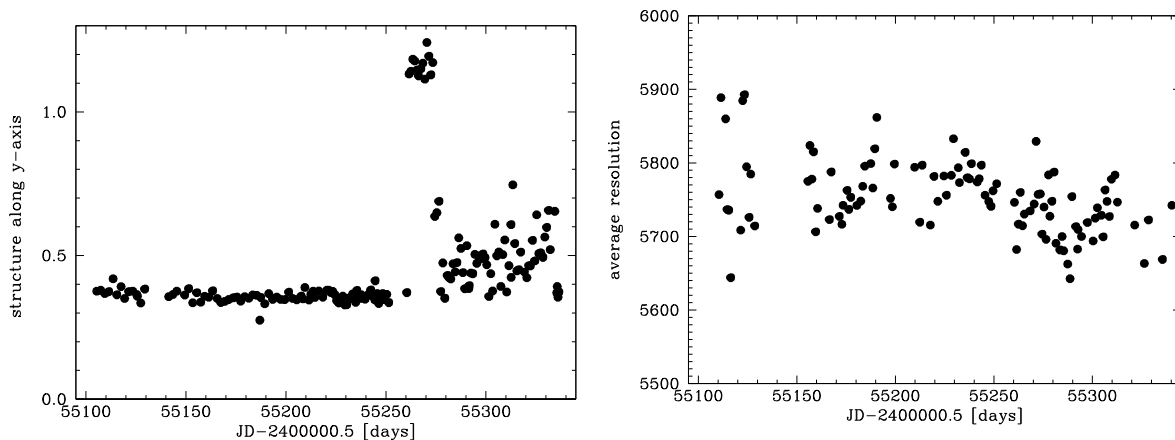
Figure 2. On the left hand panel is shown a trend plot of the VIS arm master bias Y structure. On the right hand panel a trend plot of the average resolution of the 0.9x11 slit in NIR arm is shown.

4.4 Spectral format guess

This data reduction step uses a reference catalogue of selected arc lines and either a static guess table with the locations of the corresponding lines on the detector or the physical model configuration updated to the ambient conditions at the time the spectral format frame has been acquired. Then it locates the positions of emission lines on a one-pinhole arc lamp frame, previously bias corrected (UVB,VIS) or off-lamp frame corrected (NIR) via a 2D Gaussian fit. This operation determines a first guess of the instrument spectral format: the central order traces and a first guess dispersion solution that are stored in corresponding product tables. In polynomial mode tables containing polynomial coefficients that give a guess solution for the central order traces and the wavelength dispersion solution are generated; in physical model mode an order guess table and a table containing the physical model coefficients optimised on the spectral format frame are generated. Additional products, for quality control, are a table with the residuals measuring the accuracy of the solutions (see Fig. 4, upper panel), a sub list of the input line list with the identified lines and the bias/off-frame subtracted format-check frame that can be used to over-plot the found solutions for quality control. Using the script test_data_resid_tab it is possible to generate regions files containing the locations of the predicted line positions that can be over-plot with ds9 to the format-check frame to verify the accuracy of the solutions (see Fig. 3.
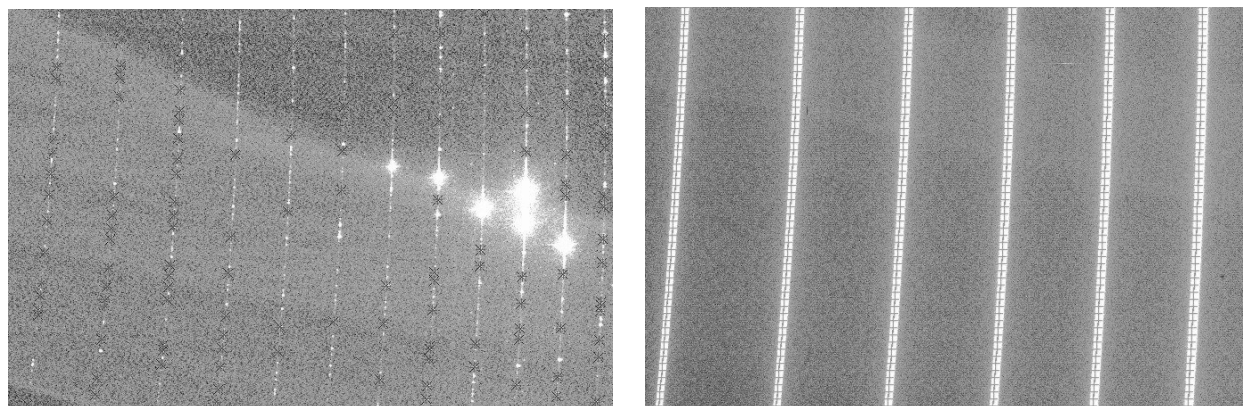

Figure 3. On the left hand side panel line predictions superimposed on a bias subtracted one-pinhole arc lamp frame are shown for quality control. On the right hand side panel the traces of the detected orders from the polynomial solution stored in the order table superimposed to a bias subtracted one-pinhole flat (continuum) lamp frame to check the accuracy of the order tracing step are shown. Both panels shows VIS arm data results.

4.5 Order flat tracing

Using the information contained in the guess order table the centroids of each spectral pixel bin on a single pinhole flat lamp exposure are determined. This allows a more accurate determination of the order central trace. The residuals measuring the accuracy of the corresponding solution are generated for quality control (see Fig. 4, bottom panel) and for each order the statistics of count levels along the order trace are computed to eventually reveal frame saturation and monitor detector responsivity. Using the script test_data_order it is possible to generate regions files containing the locations of the order traces that can be over-plot with ds9 on to the order position frame (see Fig. 3, right panel) to verify the accuracy of the order tracing.
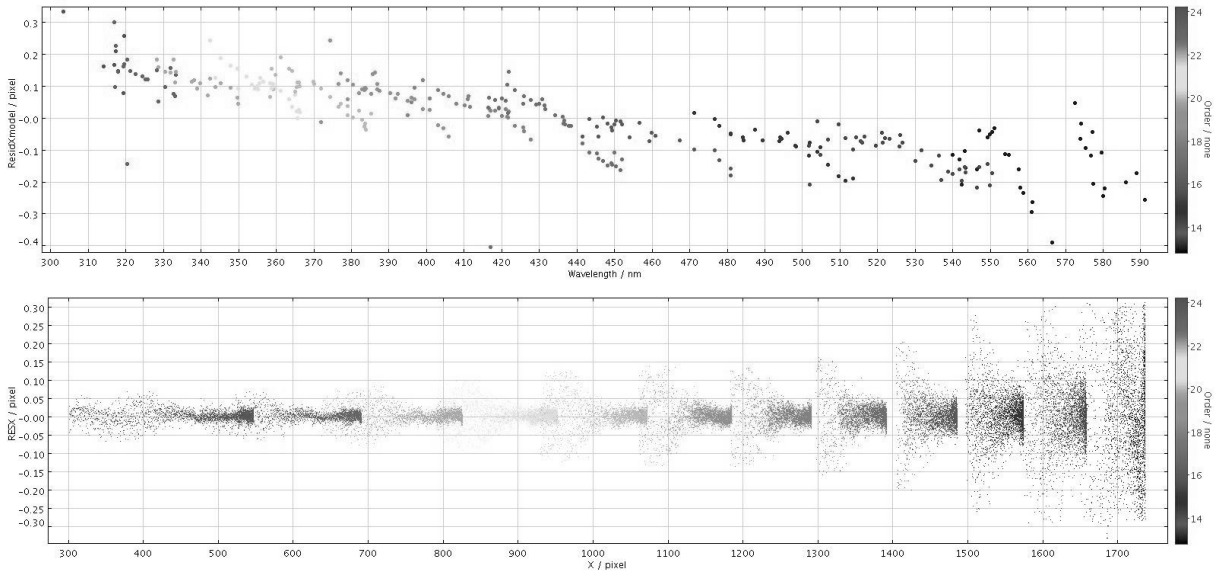

Figure 4. On the upper panel are shown the residuals corresponding to the guess solution found analysing a UVB arm single pinhole arc lamp frame. On the bottom panel are shown the residuals corresponding to the central order trace solution for a UVB arm order definition flat frame .

4.6 Slit and IFU Flat analysis

From a series of spectroscopic flat field exposures a master frame is determined via median stack with CRHs removal. For quality control the flux of the raw flats is monitored to reveal frame saturation. The flat edges are traced using a threshold of the flux at the order center (see left panel of Fig. 5 for a slit mode example). In IFU mode also the IFU slice edges are traced using the Sobel edge detection method. These edge locations are fitted by polynomial expressions and stored in the order-edges table product. These positions are used to locate inter-order regions to estimate the background level and subtract a 2D linear spline (or a 2D polynomial) fitted on the counts measured at each sampling point (see Fig. 5, right panel). For the UVB arm two different flat field lamp frames (^{2}D and QTH) are used to have a well exposed combined master frame over all orders, which combines the first four bluest orders from the $_2$D lamp frames and the others using the other lamp frames. Finally on the master flat frame the locations of dead and saturated pixels are determined and stored in corresponding maps.

4.7 Multi-pinhole frame data reduction

The guess arc lamp emission line positions coming from the format-check frame analysis (either polynomial solution or optimitized model configuration) are then used to locate via a 2D Gaussian fit the positions of each of the nine pinholes present in the input frame. The multi-pinhole line positions are used either to fit a global polynomial solution or to refine the instrument physical model configuration. This solution allows the determination of the pixel position (X, Y) for a any traced order number m, wavelength λ and position along the slit s. Then the inverse polynomial solution is calculated, that allows the determination of the wavelength
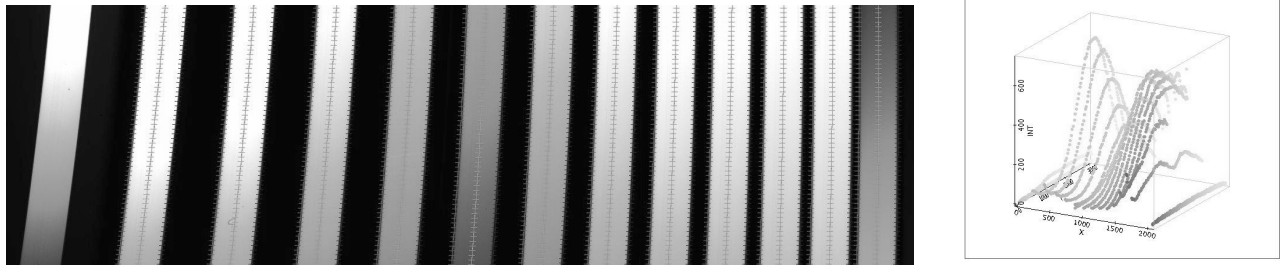
Figure 5. A master slit flat frame with edges and central traces plots to check tracing accuracy (left). The count levels measured on sampling regions distributed along inter-order regions used to estimate the inter-order background are shown (right). The images refer to UVB arm data for which the master and the background frames are obtained combining corresponding frames determined on two set of data, one using a ^{2}D lamp and the other using a QTH lamp exposures.

and slit position as a function of the detector position (X, Y). This information is used during science reduction to conserve flux when orders are rectified. Finally a wavelength and a slit map are generated either using the information from the latter polynomial expression or the physical model. The accuracy of this critical data reduction step can be checked for example using the script test_xsh_resid_tab that generates a region file that can be over-plotted to the multi-pinhole arc lamp frame, or by plotting the residual of the found solution. In Figure 6 the detected lines projected on the multi-pinhole frame (upper panel) and the corresponding Y residuals (lower panel) are shown.
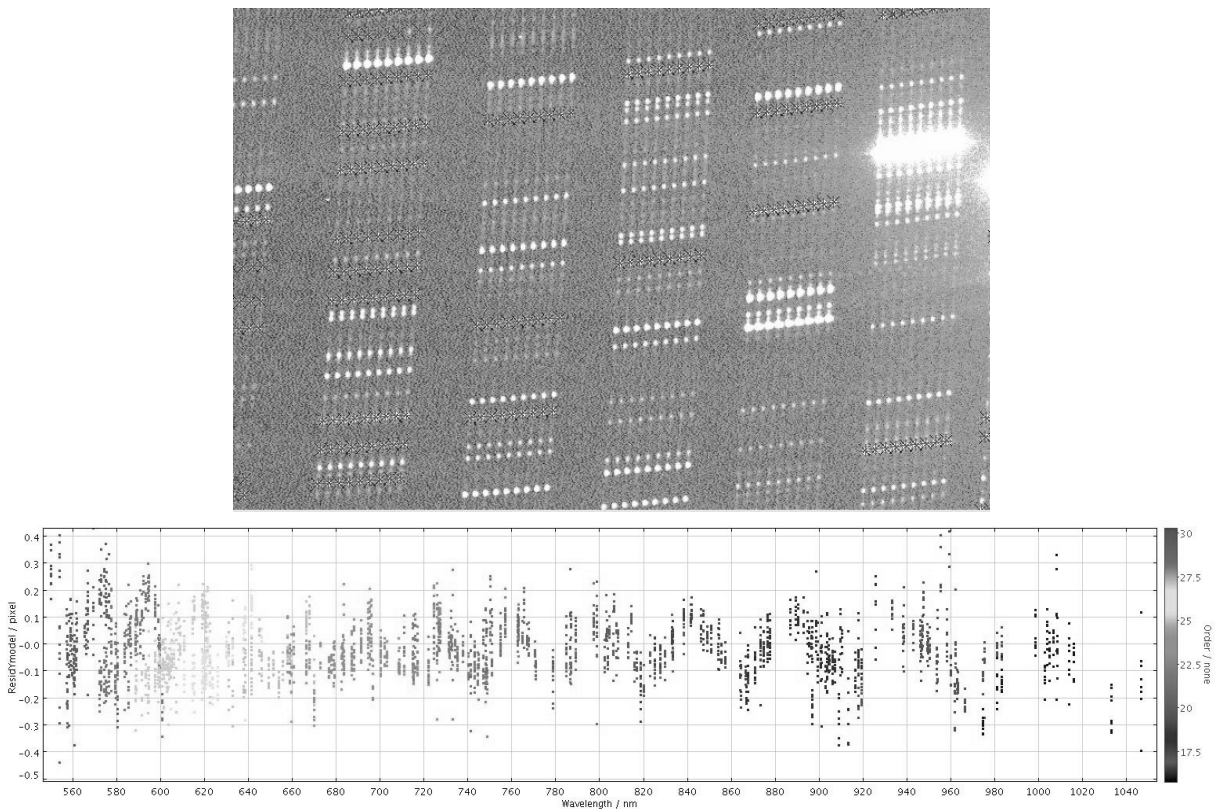

Figure 6. This image displays the detected lines projected on the multi-pinhole frame (upper panel), and the corresponding Y residuals (lower panel) .

4.8 Slit and IFU Arc frames reduction

The input data are prepared, and master bias subtracted (UVB, VIS) or off-frame corrected (NIR). The resulting frames are divided by the master flat field. Then for each order, using the solution determined after processing of the multi-pinhole frame, and a reference line catalogue, the center, FWHM and tilt of each detected line are computed. This data reduction step allows measurement of the line tilt and the instrument spectral resolution (see Fig. 2, right panel).

4.9 Instrument flexure measurement and correction

X-shooter is a massive instrument mounted at the Cassegrain focus of Kueyen. The orientation of the spectrographs varies with the zenith angle and, away from zenith, with the position angle. Flexure causes a change of the position of the object source along the entrance slit of the X-shooter spectrograph. This effect is corrected by an active flexure compensation system based on the use of piezo controlled mirrors. Moreover the flexures induce small movements of the spectrographs optical elements. This last contributes to spectral format shifts that can be corrected at least to first order by the data reduction. This is possible by the acquisition of special flexure compensation frames (a kind of attached calibration frames) before each science template. In order to reduce the detector read-out time, only 1000x1000 pixels are read-out with a very short exposure. Using the physical model (or the polynomial) solution obtained after the analysis of the multi-pinhole frame, it is possible to measure the shift of a small set of known emission lines and consequently correct the model (or the polynomial) solution. This correction is critical to obtain good accuracy in case of IFU science data reduction.

4.10 Reduction of object frames in stare mode

If there are more than two input frames, those are stacked and CRHs are removed using median stacking. After master bias (UVB, and VIS) and master dark (if available) subtraction, the inter-order background is estimated using the information given by the table tracing order edges via a spline or polynomial method, and then subtracted from the data. Next the frame may be divided by the master flat. Then the sky background may be estimated and subtracted using the method developed by Kelson.[9] If the user would like to remove CRHs in a single frame a preliminary object localization is performed in order to mask the object while the sky is estimated. This may be done manually, in which case the user specifies the information where the object is located, or automatically by employing a Gaussian fit of the object's cross order profile. CRHs are determined using the L.A. cosmic by van-Dokkum[10] after a preliminary sky estimation and subtraction. After CRHs have been removed, the sky is added back and a new object localization is performed on the cosmic ray cleaned frame. Then a final sky subtraction is performed masking the object. In Figure 7 we show results of single frame sky subtraction (right panel) compared with the frame before sky subtraction for an object having a very weak (and very few) emission line(s) spectrum. Next the frame is rectified from the pixel (X, Y) space on to a regular grid (λ, s) space. A 1D spectrum is generated by collapsing the 2D product on a range of slit positions specified by user input parameters. A merged 2D spectrum is obtained with simple or weighted mean of the overlapping order regions, and a 1D merged spectrum is obtained by collapsing the 2D product on a range of slit positions specified by user input parameters. Alternatively the 1D spectrum can be extracted with optimal extraction. In Figure 9 we show the merged 1D spectrum of a quasar over the full X-shooter wavelength range observed in stare mode in the UVB and VIS arm and nodding mode in the NIR arm.

4.11 Optimal extraction

Optimal extraction is performed on the bias, dark, inter-order background, flat-field corrected science frame. To ensure flux conservation the corrected frame is multiplied by the blaze function that is obtained with a polynomial fit of the master flat counts measured along the central order traces. The object frame, and corresponding wavelength and slit maps are over-sampled by a user defined factor. Then the extraction is performed for each order. The order is analysed at X, Y positions taken along traces (given by the polynomial solution or the physical model) parallel to the central order trace each separated from the next neighbor by the Y step size in the over-sampled space (see Fig. 8, left panel).

To each X,Y point in the super-sampled space the corresponding wavelength λ is associated using the wavemap. To this (X,Y,λ) point the lower and upper limits in the slit space are associated using the slit
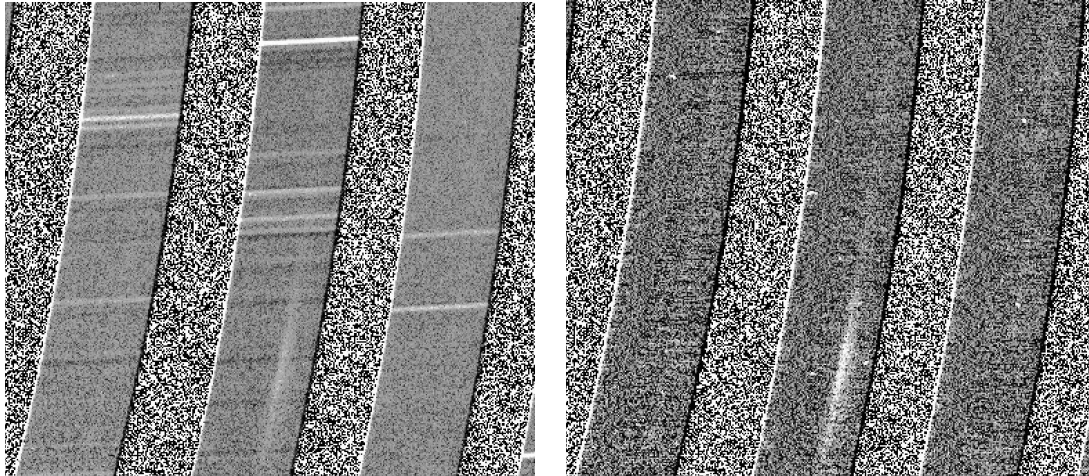
Figure 7. Results from single frame sky subtraction: MRC0943-242 is a radio-galaxy at redhift 2.92 hosting a hidden powerful AGN. In this spectrum one may see mostly narrow lines from the gas excited by the strong UV radiation from the AGN (the usual broad AGN lines are hidden). On the left hand side is shown the 2D frame after inter-order background subtraction, CRHs rejection and flat-field correction. On the right hand side the same frame after sky subtraction.
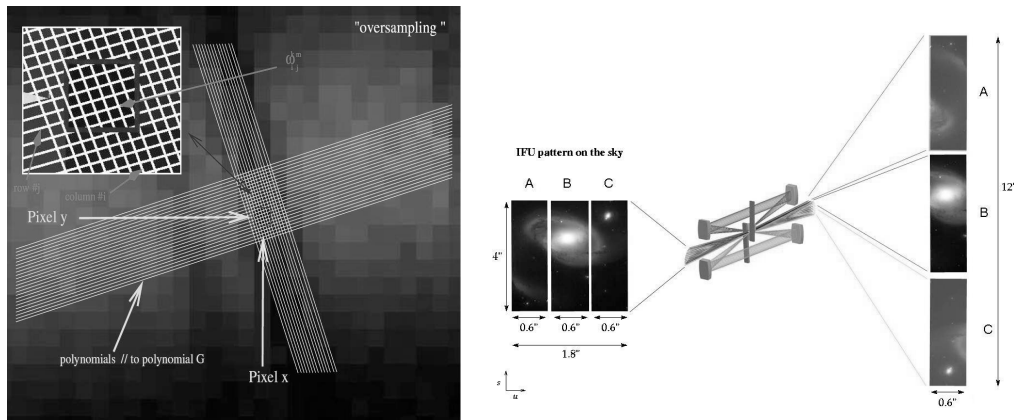

Figure 8. Left: optimal extraction geometry in the super-sampled space. Right: sketch of the IFU imaging on the slit.

map information. Using those limits it is possible to estimate the line (or slit) tilt at the order center. In order to improve speed, as the (usually point like) object does not extend over the full slit, the extraction is performed over a shorter extraction slit. Then for each X,Y the profile is determined by linear interpolation of the signal along the slit direction in the over-sampled space. This operation defines pseudo rectified orders. Those can be collapsed over a user defined slit centred on the object to define a 1D extracted spectrum. The division of the 2D pseudo-rectified orders by the 1D extracted spectrum removes spectra features.

Then the cross order profile is estimated, using either a Gaussian or a general profile. In the first case the Gaussian parameters (position, FWHM, residual background, integrated area) are obtained in different portions of the order after collapsing the order in chunks and performing a Gaussian fit to the cross profile in each chunk. Then two polynomial fits are performed to the set of positions and FWHMs values. The cross profile integrated Gaussian area is used to associate to each pixel a proper weight. Pixels contaminated by CRHs can be discarded by comparing the count levels given by the Gaussian profile approximation with the corresponding count levels of the 2D pseudo-rectified order divided by the 1D standard extracted spectrum using appropriate threshold values.

In the case of the general profile, as in the virtual re-sampling method proposed by Mukai,[11] no assumption is made on the shape of the cross order profile. The profile is approximated by polynomials along the dispersion

axis. The fluxes are estimated at sub-pixels for which the position in the original frame is closer than a given amount. These fluxes are then interpolated by polynomials in order to get an estimate of the weight at every position of the order. At this step, the interpolated values are compared with 2D pseudo rectified orders divided by the 1D standard extracted spectra in order to discard the contribution from pixels that are contaminated by CRHs.

Once extracted the orders are evenly re-sampled using the user defined wavelength sampling step.

4.12 Instrument response and efficiency determination

To compute the instrument response the 1D spectrum is integrated to obtain the same binning as the one of the reference standard star spectrum, and the atmospheric extinction is interpolated to the same binning. The table is divided by the extracted 1D spectrum and the resulting ratio is multiplied by the atmospheric extinction.

The efficiency at a given wavelength λ is computed as:

$$\epsilon(\lambda) = \frac{I_{STD}^{XSH}(\lambda) \cdot 10^{0.4 \cdot Atm\_ext(\lambda) \cdot (airp - airm)} \cdot gain \cdot E_{phot}(\lambda)}{T_{exp} \cdot A_{tel} \cdot I_{STD}^{ref}(\lambda)} \cdot factor$$

where $I_{STD}^{XSH}(\lambda)$ is the extracted standard star spectrum as observed by X-shooter, corrected for the contribution from the sky background, at a given wavelength λ, $Atm\_ext(\lambda)$ is the atmospheric extinction value, $airm$ is the airmass at which the object (star) was actually observed, $airp$ is a parameter to indicate if the efficiency is computed at airmass=0 (no-atmosphere) or at a given value (the one at which the reference standard star spectrum is tabulated). $gain$ is the detector's gain, and $E_{phot}(\lambda)$ is the energy of one photon ($E_{phot}(\lambda) = 10^7/(\lambda \cdot 1.986 \cdot 10^{19}) \cdot J \cdot \mu m^{-1}$), T_{exp} is the total exposure time in seconds, A_{Tel} is the UT telescope collecting area ($51.2 \cdot 10^4 \cdot cm^2$), $I_{STD}^{ref}(\lambda)$ is the flux calibrated spectrum of the reference source. $factor$ is a number that corrects for the fact that in the previous formula some quantity has been expressed in different units.

4.13 Reduction of observations in slit nod mode

The raw frames are composed of a series of couples with object position A and B on the slit (these positions may vary in the series if jitter is used). The input frames are initially prepared. To shorten data reduction time the recipe first co-adds all frames at the same nod position. If there are more than two A and B frames, the CRHs are removed using median sigma-clipping cleaning. Then for each nodded pair A, B, the following data reduction steps are performed.

- The frame A−B is computed to subtract the sky contribution to first order.

- In order to detect both the positive CRHs (from A) and negative ones (from B) in A−B, the frames |A−B| and sign(A−B) are computed so that $A - B = sign(A - B) \times |A - B|$.

- Then the CRHs are corrected using the L.A. cosmic algorithm on |A−B|, and the resulting frame is multiplied by the sign(A−B) frame. Next the frame A−B is divided — or not — by the master flat field. Later the frame is rectified from the pixel space (X, Y) onto a regular grid in the (λ, s) space.

- The localization is done on the rectified frame to derive the object position along the slit. This operation is done for the positive frame to derive the localization of A, and for its opposite to derive the position of B.

- The B−A frame is rectified and shifted to the position of A. In the quick look mode, the rectified B−A is taken as the opposite of A−B and shifted by an integer amount of pixels in s (it saves one rectification).

  In the normal mode, B−A is taken as the opposite of A−B after the CRH correction, and the flat field division is repeated on this frame. Then the rectification and the shift along the slit are done in a single operation to re-sample the frame only once, and the s position where the rectified flux is estimated is corrected from the shift between A and B. The shift between A and B used to shift B−A may come from the difference in the localizations or from the FITS keywords `SEQ CUMOFF RA` and `SEQ CUMOFF DEC`.
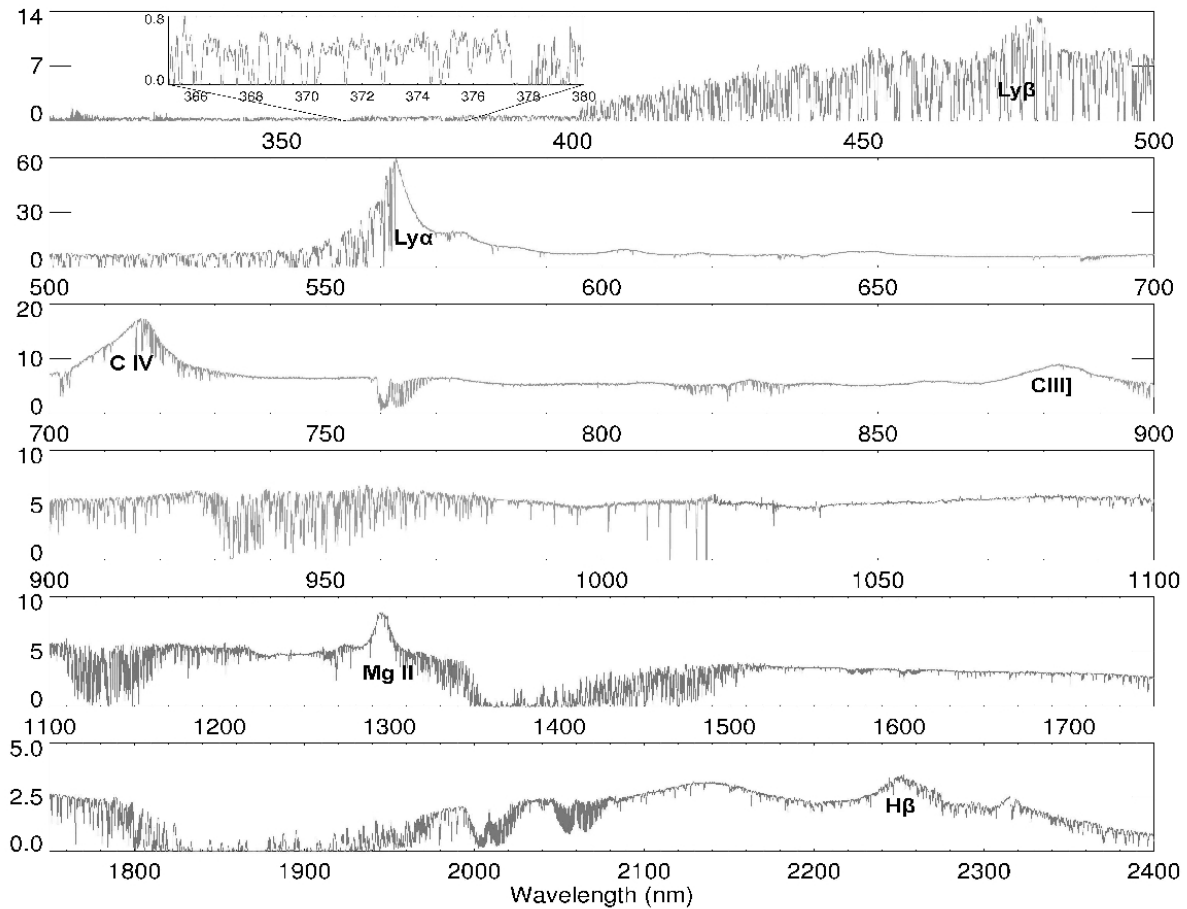
Figure 9. Spectrum of the lensed quasar B1422+231. The spectrum shows the UVB, the VIS, and the NIR data in units of 10^{-16} erg s^{-1}cm^{-1}, using different grey scales for the different portions of the spectrum. No correction for telluric lines has been applied.

Next all the rectified and shifted frames are combined together into a single frame (with a larger range in s that encompasses the "positive" and both "negative" spectra). A kappa-sigma clipping can be done during this combination. This step removes the sky contribution to second order. A 1D spectrum is produced by collapsing the 2D product on a range of slit positions specified by the input parameters.

4.14 Reduction of observations in slit offset mode

If there are more than two input frames, those are stacked and CRHs are removed using median stacking. As in the slit-nod data reduction each object and sky pair is prepared and the sky frame is subtracted to the object one. Then the inter-order background is estimated as described in slit stare data reduction and subtracted. Next CRHs detection is performed as described for slit nod data reduction where in offset mode data reduction the object and the sky play respectively the roles of the A and B frames for slit nod data reduction. The CRHs clean frame on−off is divided — or not — by the master flat. The frame is rectified from the pixel space (X, Y) onto a regular grid in the (λ, s) space. The localization is done on the rectified frame to derive the object position along the slit.

The on−off frame is rectified and shifted to the position of the first on frame. The rectification and the shift along the slit are done in a single operation to re-sample the frame only once, and the s position where

the rectified flux is estimated is corrected from the shift between the on frames. The shift may come from the difference in the localizations or from the FITS keywords `SEQ CUMOFF RA` and `SEQ CUMOFF DEC`. A 1D spectrum is produced by collapsing the 2D product on a range of slit positions specified by the input parameters.
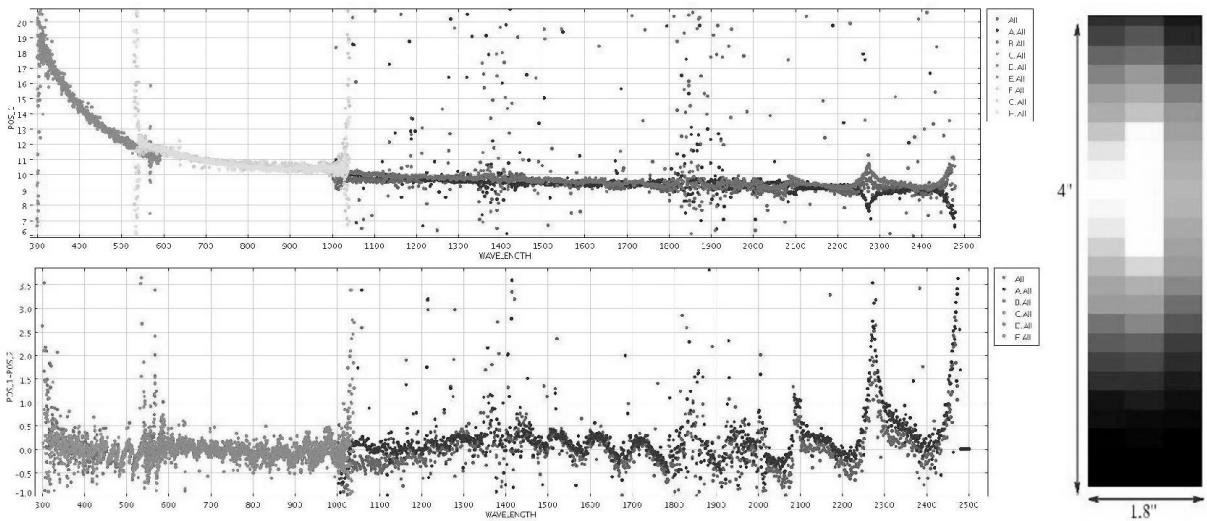

Figure 10. Upper left: combined IFU upper, central and lower traces for the three arms. The curvature is due to differential atmospheric dispersion as there is no ADC for the IFU. Lower left: residuals of lower-central and upper-central traces for a standard star used to verify accuracy. Right: a slice of the 3D cube at H_α. The spatial size of one pixel is 0.15".

4.15 Reduction of observations in ifu stare and offset mode

The input frames are prepared. If three or more science frames are present in the set-of-frames, they are combined into one median frame to reject the CRHs. The master bias frame (UVB and VIS arms), and the master dark frame (if available) are subtracted. The inter-order background is determined and subtracted. Then the frame is divided by the master flat field. The sky background is not removed from an IFU observation in staring mode.

Finally the 3D data cube is constructed. For each detected order m, wavelength λ, and slit value in the central IFU slice s^{cen}, the (x^{cen}, y^{cen}) position corresponding to the current (m, λ, s^{cen}) is determined, using either the flexure corrected global polynomial solution or the physical model. The (x^{upp}, y^{upp}) and (x^{low}, y^{low}) corresponding positions in the two adjacent IFU slices are determined using fixed calibrated relations (1) and (2). The corresponding fluxes, errors, and qualifier are determined by interpolating the pre-processed IFU science frame (and corresponding error) images. Those values are stored in the cube position corresponding to the given IFU slice, spatial and wavelength coordinate. Cube value points corresponding to wavelengths where different orders overlaps are averaged. For quality control, the recipe computes the object traces in each IFU slice (see Fig.10).

To find the relations (1) and (2) a Gaussian fit of object trace X position in each IFU slice is performed for each order and Y position constrained to a X range set by the traced IFU slices edge positions. Then each (x, y) pair found in each IFU slice is converted in corresponding (s, λ) positions using the wave and slit map information (poly mode) or the model (physical model mode). The distribution of $s^{upp}(\lambda)$, $s^{cen}(\lambda)$, $s^{low}(\lambda)$ is different, but the sum $s^{upp}(\lambda) + s^{cen}(\lambda)$, and $s^{low}(\lambda) + s^{cen}(\lambda)$, is a constant, equal to twice the distance between the slices from the optical center. The following equations are valid:

$$s^{upp} = \sigma \cdot s_{cent} + c_0^{upp} + c_1^{upp} \cdot \lambda + c_2^{upp} \cdot \lambda^2 \tag{1}$$

$$s^{low} = \sigma \cdot s_{cent} + c_0^{low} + c_1^{low} \cdot \lambda + c_2^{low} \cdot \lambda^2 \tag{2}$$

Where $\sigma = -1$ has been determined in the lab, and the coefficients c_i^{upp}, c_i^{low} ($i = 0, 1, 2$) have been determined minimizing residuals in the final cube reconstruction over a set of standard stars (see Fig. 10).

Data acquired in offset mode are reduced in the same way, with the only difference that in this case input frames are (usually low signal to noise) object and sky frames that are initially separated in object and sky pairs and the sky frame is subtracted from the object one.

5. SUMMARY AND CONCLUSIONS

We have described the X-shooter data reduction chain, main results and quality checks that allow to check the accuracy of any data reduction step and the reduction of X-shooter science data. The pipeline has already proven to be a very useful tool for checking the health of the instrument, the quality of the calibrations and science observations during X-shooter operations and to reduce X-shooter science data in the different X-shooter observing modes.

ACKNOWLEDGMENTS

REFERENCES

[1] Ballester, P., Banse, K., Castro, S., Hanuschik, R., Hook, R. N., Izzo, C., Jung, Y., Kaufer, A., Larsen, J. M., Licha, T., Lorch, H., Lundin, L., Modigliani, A., Palsa, R., Peron, M., Sabet, C., and Vinther, J., "Data reduction pipelines for the very large telescope," in [*Observatory Operations: Strategies, Processes, and Systems.*], Silva, D. R.; Doxsey, R. E., ed., *Proc. SPIE* **6270**, 6270T (2006).

[2] Silva, D. and Peron, M., "VLT science products produced by pipelines: A status report," *The Messenger* **118**, 2 (Dec. 2004).

[3] Moehler, S., Bristow, P., Kerber, F., Modigliani, A., and Vernet, J., "The physical model in action: Quality control for x-shooter," in [*Observatory Operation*], *Proc. SPIE* **7737** (2010).

[4] Goldoni, P., Royer, F., François, P., Horrobin, M., Blanc, G., Joel, V., Andrea, M., and Jonas, L., "Data reduction software of the x-shooter spectrograph," in [*Ground-based and Airborne Instrumentation for Astronomy II*], Ian S. McLean, M. I., ed., *Proc. SPIE* **6969**, 62692K (2006).

[5] Vernet, J., Dekker, H., D'Odorico, S., Mason, E., Marcantonio, P. D., Downing, M. D., Elswijk, E., Finger, G., Fischer, G., Kerber, F., Kern, L., Lizon, J.-L., Lucuix, C., Mainieri, V., Modigliani, A., Patat, F., Ramsay, S. K., Santin, P., Vidali, M., Groot, P., Guinouard, I., Hammer, J.-F., Kaper, L., Kjaergaard-Rasmussen, P., Navarro, R., Randich, S., and Zerbi, F. M., "Performance of x-shooter: the new wide-band intermediate resolution spectrograph at the vlt," in [*Observatory Operation*], *Proc. SPIE* **7735** (2010).

[6] Bristow, P. and Kerber, F., "Model based calibration," in [*ESO Calibration workshop*], (2007).

[7] Bristow, P., Kerber, F., Vernet, J., Moehler, S., and Modigliani, A., "Using the x-shooter physical model to understand instrument flexure," in [*Observatory Operation*], *Proc. SPIE* **7735** (2010).

[8] Modigliani, A., Bristow, P. D., and Izzo, C., "Reference object identification: Pattern-matching or first-guess model? a procedure to determine the spectral format of x-shooter takes advantage of both techniques," in [*Ground-based and Airborne Instrumentation for Astronomy*], David A. Bohlender, Daniel Durand, P. D., ed., *Proc. ADASS* **411**, 258 (2009).

[9] Kelson, D. D., "Optimal techniques in two-dimensional spectroscopy: Background subtraction for the 21st century," *Proceedings of Astronomycal and Science in Pacific* **115**, 688 (June 2003).

[10] van Dokkum, P. G., "Cosmic-ray rejection by laplacian edge detection," *Proceedings of Astronomycal and Science in Pacific* **113**, 1420 (Nov 2001).

[11] Mukai, K., "Optimal extraction of cross-dispersed spectra," *Astronomycal Society of the Pacific* **102**, 183 (Feb 1990).